Identifying sources of respirable quartz and silica dust in underground coal mines in southern West Virginia, western Virginia, and eastern Kentucky

Steven J. Schatzel

National Institute for Occupational Safety and Health, Pittsburgh Research Laboratory, 626 Cochrans Mill Road, PO Box 18070, Pittsburgh, PA 15236, USA

A B S T R A C T

Prior research has suggested that the source of respirable silica dust in underground coal mines is typically the immediate top or bottom lithology adjacent to the mined seam, not mineral matter bound within the mined coal bed. Geochemical analyses were applied in an effort to identify the specific source rock of respirable quartz dust in coal mines. The analyses also demonstrate the compositional changes that take place in the generation of the respirable dust fraction from parent rock material. All six mine sites were mining coal with relatively low mineral matter content, although two mines were operating in the Fire Clay coal bed which contains a persistent tonstein. Interpretations of Ca, Mg, Mn, Na, and K concentrations strongly suggest that the top strata above the mined seam is the primary source of mineral dust produced during mining. One site indicates a mixed or bottom source, possibly due to site specific conditions. Respirable dust compositional analyses suggest a direct relationship between the quantity of mineral Si and the quantity of quartz Si. A similar relationship was not found in either the top or bottom rocks adjacent to the mined seam. An apparent loss of elemental Al was noted in the respirable dust fraction when compared to potential parent rock sources. Elemental Al is present in top and bottom rock strata within illite, kaolinite, feldspar, and chlorite. A possible explanation for loss of Al in the respirable dust samples is the removal of clays and possibly chlorite minerals. It is expected that removal of this portion of the Al bearing mineral matter occurs during rock abrasion and dust transport prior to dust capture on the samplers.

1. Introduction

Overexposure to respirable quartz dust can lead to the development of silicosis, a debilitating and potentially fatal lung disease. The current federal permissible coal mining exposure limit for respirable dust in coal mines is 2 mg/m^3 (Title 30, Code of Federal Regulations, 2007). If the respirable dust sample contains more than 5% quartz, federal regulations reduce the allowable respirable dust standard the coal mine operator must meet. The reduced standard is defined as (10/silica %) mg/m^3 (Title 30, Code of Federal Regulations, 2007). In the discussion of mining-related respirable silicate mineral matter, the term "silica" has been used to include all crystalline, crypto crystalline, and amorphous forms of silica dioxide in respirable dust from all types of mines.

Compliance data show that a significant portion of roof bolter and continuous miner samples collected exceeded the federal dust standard (National Institute of Occupational Safety and Health, 2001). In samples from 2000 to 2004, 20% exceeded the MSHA reduced standard silica dust concentration of 100 μg/m^3 (Goodman, 2006). The control of quartz dust in coal mines is limited by uncertainty regarding the origins of quartz yielded in the respirable dust fraction. Results from several research studies indicate that the mined seam is not the principle source of respirable silica dust (Hicks and Nagelschmidt, 1943; Dodgson et al., 1971; Ramani et al., 1987). Clay coatings have been noted on respirable, quartz dust grains (Wallace et al., 1994; Harrison et al., 1997). The frequency of silicosis appears to increase with the presence of more toxic, clean SiO_2 quartz tetrahedra (Dodgson et al., 1971; Robock and Bauer, 1990; Chen et al., 2005; Harrison et al., 2005). A key project task for this research is to develop methodology capable of distinguishing potential top rock and bottom rock sources of the respirable silica dust fraction produced during continuous mining activities to identify the parent rock source.

2. Methodology

2.1. Study area

The locations of the six cooperating mine sites are shown in Fig. 1. The study area encompasses parts of western Virginia, southern West Virginia, and eastern Kentucky. The coal beds included a range in rank from high volatile A bituminous in Kentucky and West Virginia to medium volatile bituminous in Virginia. All mines are drift, room and pillar operations and are using on the order of 14 m^3/s of ventilation air at the last open cross cut. The positional data and the coal bed names for the cooperating mines are given in Table 1. More detailed information on the study sites is contained in Appendix A.

E-mail address: zia6@cdc.gov.

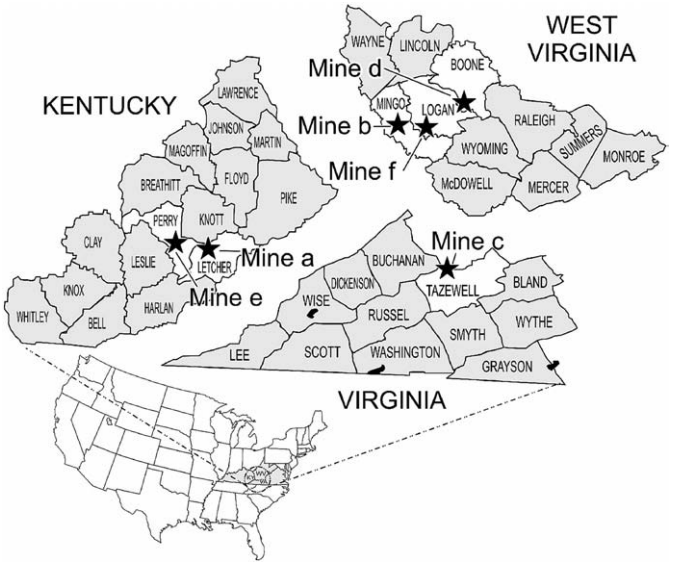

Fig. 1. The location of mine sites included in this study.

2.2. Field sampling

The protocol developed in this study called for sampling of rock and coal from known sites of at current production sections and in previously mined locations where high quartz concentrations were determined in respirable dust. Samples of overburden rock immediately overlying the coal bed and samples of underlying bottom rock were retrieved. These rock strata are referred to as top and bottom rock respectively and make up what the coal mining industry commonly refer to as "roof" and "floor" rock. Lump samples of coal were retrieved from rib locations after removal of the top 3 cm of surface coal. Lump samples of coal, top and bottom were also retrieved from operating sections. Rock binders or apparent mineralized zones occurring within the mined coal bed were also sampled.

Dust sampling was also conducted on the selected continuous miner production sections. Sampling was conducted at one intake and one return location at each mine. An exception was Mine E where two return locations were used for comparison of the dust compositional changes with distance from the miner. Conventional personal dust samplers, 10-mm nylon cyclones and 37-mm filter cassettes, were used for all sampling. The samplers were operated at 2.0 L/min. Two dust samplers were utilized at each sampling location.

2.3. Analytical methods

Masses of all dust samples were measured in the Respiratory Hazards Control Branch (RHCB) weighing laboratory at NIOSH. A set of dust filter cassettes was used for analysis by X-ray fluorescence (XRF), a non-destructive, semi-quantitative method giving elemental composition of major cations on the filters. Following XRF analysis, the

Table 1
Geographic positioning system (GPS) coordinates for locations near the portals of the six coal mine study sites

Mine site	State	Latitude	Longitude	Coal bed
A	Kentucky	nd[a]	nd[a]	Fire Clay
B	West Virginia	N37° 43.456′	W081° 59.747′	Williamson
C	Virginia	N37° 11.488′	W081° 43.007′	Lower Horsepen
D	West Virginia	N37° 54.389′	W081° 34.071′	Powellton
E	Kentucky	N37° 10.3821′	W083° 11.737′	Fire Clay
F	West Virginia	N37° 44.632′	W082° 12.240′	Lower Cedar Grove

[a] Not determined.

Table 2
X ray diffraction results

Sample type	Top	Top	Bottom	Top	Top	Bottom	Bottom	Top	Bottom	Top	Coal binder	Bottom	Top	Top	Bottom
Mine	A	A	A	C	C	C	D	E	D	E	E	E	F	F	F
Mineral species	arock4top	arock11top	arock10bot	crock3top	crock6top	crock1bot	drock5top	drock6top	drock3bot	drock6bot	erock6top	erock7coal	erock5bot	frock2top	frock6top	frock1bot
		%														
Quartz	27	30	44	23	38	16	50	37	59	26	37	1	28	37	31	33
Kaolinite	4	6	8	0	0	0	7	4	2	15	4	95	57	4	4	63
Illite	43	36	17	49	19	62	34	40	29	48	40	bd[a]		33	43	
Albite	9	12	19	17	5	14	6	9	5	11	9	bd[a]	13	10	10	bd[a]
Chlorite	18	16	11	10	1	4	bd[a]	10	bd[a]	bd[a]	10	bd[a]	1	16	12	bd[a]
Hematite	bd[a]	bd[a]	bd[a]	bd[a]	bd[a]	bd[a]	bd[a]	bd[a]	bd[a]	bd[a]	bd[a]	bd[a]	bd[a]	bd[a]	bd[a]	bd[a]
Pyrite	bd[a]	bd[a]	bd[a]	bd[a]	19	bd[a]	bd[a]	bd[a]	bd[a]	bd[a]	bd[a]	bd[a]	bd[a]	bd[a]	bd[a]	bd[a]
Siderite	bd[a]	bd[a]	bd[a]	bd[a]	18	bd[a]	bd[a]	bd[a]	bd[a]	bd[a]	bd[a]	bd[a]	bd[a]	bd[a]	bd[a]	bd[a]
Calcite	bd[a]	bd[a]	bd[a]	bd[a]	bd[a]	bd[a]	bd[a]	bd[a]	bd[a]	bd[a]	bd[a]	bd[a]	bd[a]	bd[a]	bd[a]	bd[a]
Ankerite	bd[a]	bd[a]	bd[a]	bd[a]	bd[a]	bd[a]	bd[a]	bd[a]	bd[a]	bd[a]	bd[a]	bd[a]	bd[a]	bd[a]	bd[a]	bd[a]
Bassinite	bd[a]	bd[a]	bd[a]	bd[a]	bd[a]	bd[a]	bd[a]	bd[a]	bd[a]	bd[a]	bd[a]	bd[a]	bd[a]	bd[a]	bd[a]	bd[a]
Organic	0	1	2	1	1	5	0	0	6	1	0	3	0	0	0	4

[a] Below detection.

Table 3
Petrographic characterization of coal samples from six coal mine study sites

Mine	A	A	B	C	C	D	D	E	E	F	F
Sample number	arock1coal	arock2coal	brock2coal	crock5coal	crock2coal	drock7coal	drock8coal	erock2coal	erock7coal	frock8coal	frock12coal
Basis		%									
Telinite	21.2	12.6	17.8	5.0	7.0	10.0	19.4	37.2	23.2	21.2	5.4
Collotelinite	23.0	22.0	33.6	27.4	35.2	25.2	36.4	22.4	24.0	45.4	4.6
Vitrodetrinite	0.6	0.6	0.2	0.8	1.0	1.4	1.0	0.6	0.2	0.4	0.0
Collodetrinite	41.8	24.8	21.2	35.4	30.2	23.8	17.4	20.6	32.4	13.8	9.2
Corpogelinite	2.6	3.2	4.2	0.8	0.4	1.6	1.8	2.6	4.6	2.0	2.6
Fusinite	0.6	10.6	4.4	9.4	10.2	19.4	5.2	2.4	3.6	3.4	21.0
Semifusinite	1.6	6.0	5.0	18.6	15.2	6.8	7.6	4.0	4.0	4.6	25.8
Micrinite	1.6	3.2	3.4	1.4	0.8	4.2	2.8	3.8	2.4	1.4	6.0
Macrinite	0.0	0.0	0.0	0.0	0.0	0.0	0.2	0.0	0.0	0.0	0.0
Inertodetrinite	0.2	1.2	0.2	1.2	0.0	1.0	0.8	0.0	0.2	0.2	0.8
Funginite	0.0	0.0	0.0	0.0	0.0	0.0	0.0	0.0	0.0	0.0	0.0
Secretinite	0.0	0.0	0.0	t[a]	0.0	0.0	t[a]	0.0	t[a]	0.0	t[a]
Sporinite	5.6	14.8	8.2	0.0	0.0	5.4	6.8	5.6	4.8	7.0	22.6
Cutinite	0.6	0.6	0.6	0.0	0.0	1.2	0.6	0.2	0.6	t[a]	1.0
Resinite	0.6	0.2	1.0	0.0	0.0	t[a]	0.0	0.6	t[a]	0.6	1.0
Liptodetrinite	0.0	0.2	0.2	0.0	0.0	0.0	0.0	0.0	0.0	0.0	0.0
Alginite	0.0	0.0	0.0	0.0	0.0	0.0	0.0	0.0	0.0	0.0	0.0
Total vitrinite	89.2	63.2	77.0	69.4	73.8	62.0	76.0	83.4	84.4	82.8	21.8
Total liptinite	6.8	15.8	10.0	0.0	0.0	6.6	7.4	6.4	5.4	7.6	24.6
Total inertinite	4.0	21.0	13.0	30.6	26.2	31.4	16.6	10.2	10.2	9.6	53.6
Total maceral groups	100.0	100.0	100.0	100.0	100.0	100.0	100.0	100.0	100.0	100.0	100.0
Rmax	0.90	0.92	0.94	1.17	1.22	0.73	0.80	0.85	0.96	1.01	0.88
Standard deviation	0.07	0.05	0.06	0.17	0.09	0.08	0.06	0.05	0.06	0.05	0.06
Rrandom	0.83	0.85	0.91	1.14	1.19	0.69	0.75	0.83	0.91	0.95	0.83
Standard deviation	0.07	0.05	0.06	0.09	0.09	0.08	0.05	0.05	0.05	0.06	0.06

[a] Trace.

filters were analyzed by the MSHA P-7 standard Fourier transfer infrared (FTIR) analysis for the determination of quartz content in the dust sample.

To compare dust samples to the rock samples, geochemical and mineralogical analyses were performed. The elemental composition of the rock samples was determined by inductively coupled plasma-atomic emission spectroscopy (ICP-AES). Low-temperature ashing (LTA) techniques were utilized to remove organic matter from the samples, and preceeded semi-quantitative XRD using internal standards mixed into the samples. See Appendix A for a detailed discussion of the analytical methods.

3. Results and discussion

3.1. Mineral analysis

Three XRD analyses were conducted for each mine site (Table 2). Quartz concentrations determined range widely from 1% in a clay binder at mine E to 50% in the top rock at mine D (Table 2). Quartz contents in the top and bottom units shown in Table 2 both average 34%. Illite concentrations exceed kaolinite concentrations and range from 17% in the bottom of Mine A to 62% in the bottom of Mine C. Kaolinite and illite were not distinguished in two samples, one from Mine E, and one from Mine F, where the sum percentage of kaolinite plus illite is shown. The averaged total aluminosilicate contents reported (illite plus kaolinite) are slightly higher for the bottom rock samples compared to the top samples, 50 and 41%, respectively.

Reported albite concentrations are quite high, reaching a maximum of 19% in a top sample from Mine A, and a minimum concentration of below detection limits (~5 to 10%) in samples from Mines D, E, and F. The lab reported that albite values could actually represent concentrations of different or mixed feldspar species, and thus is referred to as feldspar content in the remainder of this report. The averaged feldspar content of bottom and top samples shown in Table 2 is identical, 11%. Pyrite and siderite concentrations were reported from only one sample from mine C (Table 2). Chlorite is much more abundant in the top rock samples compared to bottom rock samples. Chlorite is typically an epigenetic mineral and its mode of

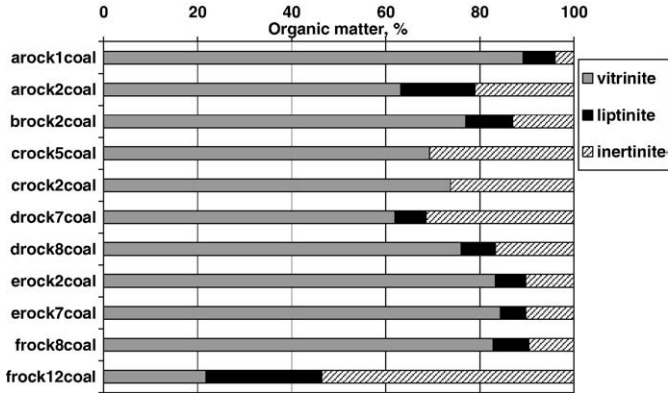

Fig. 2. The distribution of organic matter maceral groups in petrographic samples from all six mine sites.

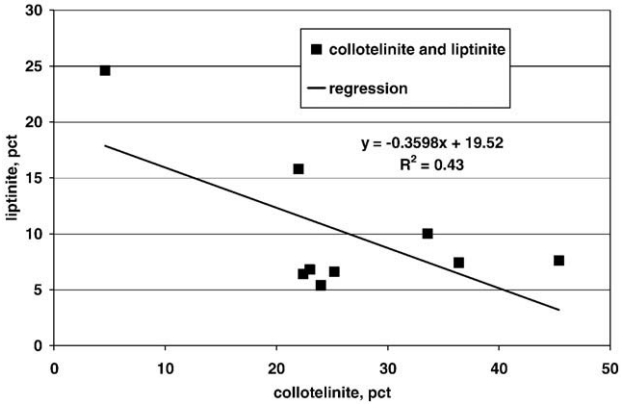

Fig. 3. A low R^2 value was determined for the trend line fit to the submaceral collotelinite and liptinite maceral group concentrations.

Table 4
ICP-AES major cation analysis data for overlying and underlying rock unit samples

			Oxide								
			SiO_2	Al_2O_3	Fe_2O_3	CaO	MgO	MnO	Na_2O	K_2O	TiO_2	P_2O_5
Mine	Sample number	Sample type		%								
A	arock4top	Top	54.38	20.38	7.42	0.60	2.14	0.097	1.18	4.93	0.931	0.18
A	arock7top	Top	57.47	18.89	7.16	0.91	2.09	0.094	1.32	4.39	1.009	0.20
A	arock9top	Top	56.96	21.63	5.98	0.29	1.91	0.059	1.19	5.36	0.931	0.19
A	arock11top	Top	58.65	19.82	6.24	0.38	1.86	0.074	1.28	4.84	0.878	0.19
A	arock11Atop	Top (duplicate)	58.46	19.75	6.23	0.37	1.86	0.074	1.29	4.83	0.876	0.18
A	arock3bot	Bottom	67.62	16.78	2.94	0.08	1.05	0.020	1.49	3.45	0.902	0.04
A	arock6bot	Bottom	58.59	22.09	4.44	0.12	1.68	0.027	1.07	5.14	1.061	0.04
A	arock10bot	Bottom	72.91	14.71	2.63	0.09	0.93	0.020	1.79	2.90	0.886	0.06
A	arock12bot	Bottom	76.44	11.93	1.92	0.23	0.61	0.014	1.91	2.39	0.722	0.18
B	brock3top	Top	56.38	21.52	6.18	0.27	1.99	0.066	0.48	4.93	0.913	0.14
B	brock4top	Top	52.29	18.25	11.50	0.69	2.10	0.200	0.59	4.03	0.824	0.18
B	brock7top	Top	54.86	18.06	10.42	0.72	2.11	0.153	0.23	3.76	0.935	0.22
B	brock8top	Top	63.65	21.24	2.01	0.08	0.85	0.007	0.35	3.63	1.582	0.03
B	brock8Atop	Top (duplicate)	62.81	21.00	1.98	0.08	0.84	0.005	0.37	3.57	1.560	0.03
B	brock1bot	Bottom	50.25	23.67	4.67	0.09	1.81	0.027	0.37	4.67	0.882	0.04
B	brock6bot	Bottom	62.56	20.59	2.46	0.09	0.80	0.005	0.35	2.53	1.535	0.04
C	crock3top	Top	57.99	21.37	5.01	0.2	1.99	0.039	0.21	5.9	0.83	0.09
C	crock8top	Top	33.9	6.31	31.64	1.48	1.07	1.058	0.5	1.59	0.357	0.3
C	crock1bot	Bottom	54.27	24.11	2.95	0.15	1.4	0.015	0.3	6.83	0.92	0.04
C	crock7bot	Bottom	66.28	17.42	3.11	0.11	1.15	0.02	0.18	4.62	0.926	0.04
D	drock2top	Top	54.2	19.55	8.66	0.39	2.0	0.174	0.24	4.56	0.844	0.14
D	drock5top	Top	63.23	7.49	14.43	0.73	1.49	0.326	0.71	1.38	0.404	0.09
D	drock1bot	Bottom	65.81	19.44	1.49	0.09	0.6	0.006	0.18	3.22	1.326	0.04
D	drock3bot	Bottom	73.97	11.96	1.32	0.05	0.47	0.005	0.18	2.57	1.791	0.03
D	drock6bot	Bottom	60.7	23.48	1.77	0.1	0.81	0.006	0.21	4.15	1.317	0.04
E	erock4top	Top	71.09	11.36	4.04	1.77	1.31	0.055	1.34	1.91	0.933	0.19
E	erock6top	Top	59.56	14.66	8.81	1.1	1.81	0.162	1.12	3.01	0.887	0.16
E	erock3bot	Bottom	71.61	15.83	1.51	0.04	0.71	0.005	0.3	4.08	1.443	0.04
E	erock5bot	Bottom	43.53	32.66	0.8	0.22	0.22	0.005	0.37	0.46	0.983	0.1
F	frock2top	Top	57.00	20.77	6.84	0.44	2.05	0.096	0.73	0.14	0.950	0.14
F	frock4top	Top	56.68	21.18	5.92	0.26	2.05	0.067	0.60	0.14	0.990	0.14
F	frock11top	Top	52.23	24.58	6.77	0.26	1.93	0.117	0.66	0.15	0.912	0.15
F	frock16top	Top	59.31	18.00	7.15	0.51	1.82	0.107	1.07	0.18	1.053	0.18
F	frock18top	Top	42.68	16.12	19.04	0.84	2.16	0.335	0.52	3.47	0.713	0.20
F	frock1bot	Bottom	67.15	18.84	1.40	0.13	0.55	0.009	0.30	0.04	1.241	0.04
F	frock3bot	Bottom	66.95	19.35	1.55	0.08	0.65	0.007	0.25	0.04	1.333	0.04
F	frock14bot	Bottom	51.09	24.15	4.50	0.10	1.87	0.030	0.38	0.04	0.956	0.04
F	frock19bot	Bottom	68.92	16.94	1.65	0.14	0.68	0.005	0.17	3.53	1.690	0.03

Analyses of duplicate samples prepared and analyzed by the lab are shown with the same sample number except for an "A" in the name before the top or bottom suffix.

occurrence may range from a fine, highly dispersed, mineral matter to cleat infillings.

3.2. Coal analysis

Vitrinite is the dominant maceral group with concentrations that vary widely from 21.8% to 89.2% (Table 3). Liptinite and inertinite contents also vary widely from 0.0% to 24.6% and from 4.0% to 53.6%, respectively. Fig. 2 shows the maceral group concentrations for each mine site. Petrographic data show a complete lack of liptinite macerals from the Lower Horsepen coal bed sample, Mine C. This sample also has the highest vitrinite reflectance value which is the most likely cause for the lack of identifiable liptinite macerals. Liptinite maceral concentrations determined in previous studies correlate well with macerals and maceral groups associated with high degrees of weathering and potential surface exposure of the organic material (International Committee for Coal Petrography, 2001). From Fig. 3, it can be seen that the total liptinite maceral group concentrations are generally inversely proportional to the collotelinite submaceral group concentrations. However, the R^2 value shows a relatively low fit quality between the trend line and the data. The lack of a more statistically significant inverse relationship may be the product of grab sampling procedures instead of

Table 5
Dust filter XRF data

Mine	A	B	C	C	D	D	D	E	E	E	E
Sample no.	421963	422003	458582	458583	483590	483594	483597	483595	483598	483600	483601
Oxide	%										
SiO_2	39.91	37.27	31.65	34.07	17.50	17.88	18.07	46.11	53.46	43.35	44.16
Al_2O_3	2.92	2.93	2.08	2.24	0.43	0.52	0.56	2.82	3.25	2.87	2.87
Fe_2O_3	1.88	1.73	1.06	1.20	2.63	2.45	2.46	0.90	1.01	0.77	0.80
CaO	0.33	0.42	0.23	0.22	0.00	0.00	0.00	0.96	1.27	0.78	0.79
MgO	1.84	1.64	1.62	1.69	1.55	1.46	1.52	1.30	1.47	1.12	1.13
MnO	0.25	0.19	0.00	0.12	0.36	0.31	0.26	0.11	0.12	0.09	0.08
Na_2O	0.91	0.23	0.29	<0.02	1.92	1.52	2.00	0.98	1.19	0.88	0.88
K_2O	6.64	5.43	5.03	6.74	10.84	5.23	9.10	4.75	6.27	4.90	4.94
TiO_2	1.18	1.33	0.60	0.68	0.00	0.00	0.00	1.12	1.36	1.23	1.26
P_2O_5	1.42	0.12	0.93	1.66	6.70	2.99	5.51	0.67	1.17	0.40	0.36

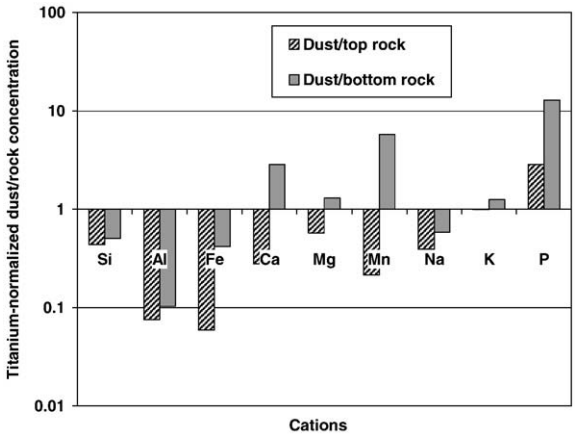

Fig. 4. Titanium-normalized dust concentrations are shown divided by Ti-normalized rock concentrations.

channel sampling methods or documented transitions of the depositional mires between planar/rheotrophic and raised/ombrotrophic settings in the coal beds (Cecil et al., 1985; Eble and Grady, 1990; Martino, 1996; Greb et al., 1999; Bodek and Eriksson, 2005).

3.3. Dust source rock analyses

Although a geochemical analysis is proposed as a method of analyzing respirable dust contributions from silica sources, there are certain limitations to the proposed technique. The application of conventional geochemistry mixing equations has not been sought since the materials being analyzed at the mine site are not conserved. For example, a portion of the coal characterized is removed as mined material. Other non-conservative processes include the disaggregation of rock material, entrainment of dust in ventilation air, followed by the transport and capture of a portion of the airborne dust in the 1 to 10 μm size fraction on cyclone samplers. Therefore, geochemical analyses are applied as an indicator or tracer to link the respirable dust to the parent rock.

Elemental analyses of rock samples (ICP-AES data set, Table 4) and the dust samples (XRF data set, Table 5) are shown. In an effort to link weathered, ancient soils to their parent rock, researchers have used Al or Ti normalization techniques (Maynard, 1992; Ohmoto, 1996; Rye and Holland, 1998; Bohn et al., 2002). A similar approach has been used in this study to determine the most appropriate cations to use in identifying the parent rock for the respirable dust samples. In Fig. 4, the concentration data for dust samples are divided by the determined Ti concentrations. These values are then divided by Ti-normalized top and bottom rock sample data (Fig. 4). The graph provides an indicator of how much the dust sample concentrations are modified from the rock sample concentrations at the time of deposition in addition to compositional changes occurring during rock abrasion, dust transport, and sampling.

Problems may exist in applying Fe and Al data to identify the respirable dust parent rock. In Fig. 4, Al, Fe and P data show the greatest difference between the Ti-normalized dust and rock data for either top or bottom rock data. Iron is present in pyrite and siderite above detection limits in only one rock sample (Table 2). In low mineral matter coals, excess Fe may be organically combined and thus not detected by XRF (Tuttle, 1990). Table 6 presents a series of elemental and oxide ratios calculated for each mine site. The dust SiO_2/Al_2O_3 ratios bear no resemblance to either the top or bottom rock and are not representative of typical sandstones or shales (Horn and Adams, 1966; Gromet et al., 1984). Table 6 also shows TiO_2/Al_2O_3 data where the respirable dust fraction shows an enrichment of Ti oxide relative to the potential parent rocks and an apparent loss of Al-bearing mineral matter. Consequently, Ca, Mg, Mn, Na, and K were chosen for the source rock analysis of respirable dust samples.

Fig. 5 shows dust sample concentrations for Ca, Mg, Mn, Na, and K normalized using top and bottom rock concentration data. To perform the normalization, cation concentrations shown for respirable mine dust were divided by cation concentrations determined for the retrieved rocks samples (Fig. 4a through e). Also included is a reference line at $y=1$ where the dust to rock ratio is one, an ideal correlation between the rock and dust data. Error bars are included in plots for the 5 mine sites. The Mine A data is shown in Fig. 5a. The Ca, Mg, and Mn data for the top rock samples are all closer to ideal correlation line than the bottom rock sample data although only the Mn data values are significantly different, based on error bar dimensions. The Mg/Ca ratios for Mine A show just a slightly stronger correspondence between the dust and top rock values. The Na/Ca data show a close correspondence between the dust and the top rock at all mine sites.

Willett et al. (2000) reported Mn to be primarily associated with carbonate with lesser amounts in aluminosilicates, sulfides and organic matter. In the same study, Ca was found to occur dominantly within the carbonate mineralogy. For the other alkali and alkaline earth elements, Willett et al. (2000) reported Mg occurs in carbonates and silicates, Na is present in aluminosilicates and exchangeable cations, and K is dominantly present in aluminosilicates. Although no carbonate mineralogy was detected by XRD, low concentrations of carbonate that are widely dispersed could be present below XRD detection limits. Ward (2002) reported that carbonate and clay components of coal mineralogy may be commonly present as epigenetic minerals. Late phase epigenetic mineralization may account for the presence of clay and low concentrations of carbonate with associated alkali and alkaline earth minerals plus Mn with less efficient fluid transport to the bottom rock strata underlying the coal beds in this study (Schatzel, 2001; Schatzel and Stewart, 2003).

Data from Mine B are shown in Fig. 5b. The Ca and Mn data for the top rock samples are much closer to the ideal correlation line than the bottom rock samples and a significant difference is shown between the two sources of rock sample data. The Mg data for the top rock sample show enrichment compared to the bottom rock sample data (closer to the $y=1$) but are not statistically different. Data for Mine C do not show the Ca and Mn dust concentrations to be similar (near $y=1$) to either the top or bottom rock samples (Fig. 5c). The Ca and

Table 6
Elemental and oxide ratios for rock and dust samples

Sample site	Sample type	Mg/Ca	Na/Ca	SiO_2/Al_2O_3	TiO_2/Al_2O_3
Mine A	Top	3.10	2.37	2.82	0.0465
	Bottom	6.93	12.5	4.21	0.0545
	Dust	4.75	2.87	13.7	0.404
Mine B	Top	3.11	0.803	2.50	0.0462
	Bottom	11.2	4.31	2.69	0.0610
	Dust	3.30	0.579	12.7	0.455
Mine C	Top	1.54	0.439	3.32	0.0429
	Bottom	8.27	1.92	2.90	0.0444
	Dust	6.22	0.662	15.2	0.297
Mine D	Top	2.63	0.88	4.34	0.0462
	Bottom	6.61	2.47	3.65	0.0221
	Dust	bd[a]	bd[a]	35.3	bd[a]
Mine E	Top	0.917	0.890	5.02	0.0699
	Bottom	3.02	2.67	2.37	0.0500
	Dust	1.05	1.01	15.8	0.422
Mine F	Top	3.66	1.85	2.70	0.0457
	Bottom	7.03	2.54	3.21	0.0658
	Dust	nd[b]	nd[b]	nd[b]	nd[b]
Average sandstone values[c]		0.665	0.326	3.83	0.0414
Average shale values[d]		0.556	0.123	3.36	0.0551

[a] Below detection.
[b] Not determined.
[c] Horn and Adams (1966).
[d] Gromet et al. (1984).

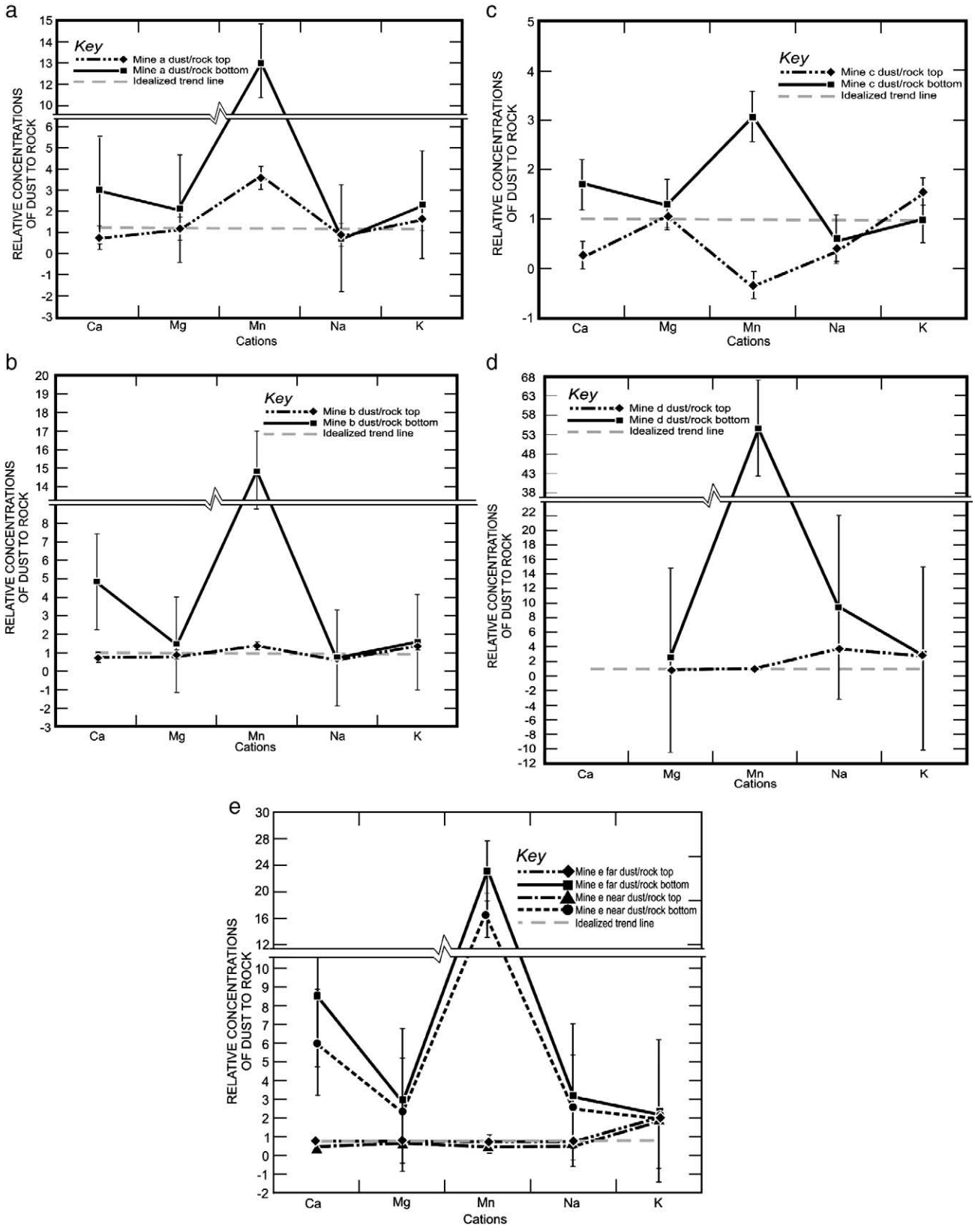

Fig. 5. Elemental ratios for Ca, Mg, Mn, Na and K determined from rocks and dust samples retrieved from Mines A through E. Vertical scales are variable.

Mn data for top and bottom rock are shown to be statistically different but about equidistant from $y=1$ and thus indeterminate regarding the likely source of the dust. The Mg, Na, and K data differences between the top and bottom rock samples do not exceed the calculated errors. Continuous miner downtime limited dust sampling at Mine C. Also, the evidence of bottom rock being cut in the production section could

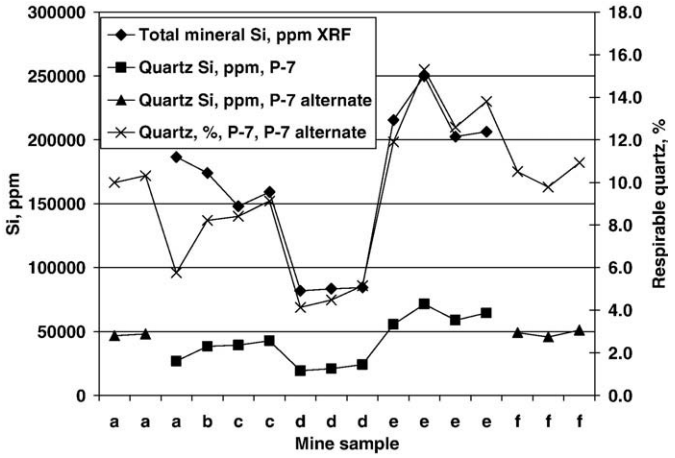

Fig. 6. Quartz and elemental silicon concentrations are shown from respirable dust samples as determined by P-7, P-7 alternate and XRF techniques.

account for a mixed top and bottom rock source for the sampled dust. Table 6 shows the Mg/Ca ratios for the bottom rock at Mine C to be closer to the dust values although the Na/Ca data show a close correspondence between the dust and the top rock.

For Mine D, the continuous miner production problems also affected the dust data set such that no Ca data are included in the plot (Fig. 5d). As in Fig. 5a and b, the plot shows Mn data for the top rock samples are much closer to the ideal correlation line than the bottom rock samples and the error calculations show these to be distinct data sets. The Mg, Na, and K data show the top and bottom rock samples to be not statistically distinct but the Mg and Na data from the top rock samples are closer to the $y=1$ line (Fig. 5d). In Fig. 5e, Mine E data shows the Ca, Mg, Mn and Na for the top rock samples results all to more closely approach the ideal correlation line than the bottom rock values, although only the Ca and Mn rock data sets are statistically distinct.

No Mine F dust cassettes were preserved for XRF elemental analysis. Rock samples from Mine F analyzed by XRD (Table 2) show potential quartz dust sources in both the top and bottom rock strata. Coal height at the working face was measured to be 0.85 m but the mining height away from the face was 1.4 to 1.9 m. Nearly all non-coal material being removed at these sites was from the top strata. Since 0.65 to 0.85 m of rock material is removed from the top strata and minimal or no rock removal from the bottom strata, the top rock is considered the most likely source rock for respirable silica dust at Mine F.

Fig. 6 shows quartz and Si dust compositional data associated with the P-7 analysis, P-7 alternate analysis, and XRF. The P-7 and P-7 alternate analysis results show the quartz contents determined on the filters. Silicon concentrations for the quartz mineral matter fraction were calculated from the P-7 and P-7 alternate analysis. The XRF data provide determinations of Si concentrations from all mineral matter sources present on the filters. For the Mine A samples, the P-7 method averaged about 6% quartz and the P-7 alternate method yielded about 10% quartz for duplicate samples splits (Fig. 6).

The graph in Fig. 6 suggests a good correspondence between total Si concentrations determined in the mineral matter on the dust filter and Si concentrations as respirable quartz. This result may be surprising since a variety of Si sources are present in the top and bottom rock samples (Table 2). The data shown in Fig. 6 are derived from all six mines which include a range of stratigraphic settings. The Fire Clay coal bed (Mines sites A and E) contains a prominent tonstein ash layer which altered during peat development and coal diagenesis (Hower et al., 1999).

To further explore the relationship between the total silica and quartz silica origins in the respirable dust samples, elemental data for the top, bottom and dust samples are plotted in Fig. 7. The dust data produce a relatively flat slope and a relatively high R^2 value of 0.79. The relatively flat slope and high R^2 suggest significant contributions of Si are present in addition to quartz and that they are contributing to the respiratory dust fraction at a relatively consistent rate at the different mine sites.

The apparent loss of Al-bearing minerals shown (Fig. 4, Table 6) is thought to be produced by the breakage, entrainment, and capture of the respirable dust particles. This process is likely to be influenced by the mineralogical composition of the Al- and Si-bearing dust fraction. Quartz and feldspar grains are harder than clays and tend to form equant fragments upon breakage whereas kaolinite, illite and possibly chlorite can form long or platy fragments and are not mechanically strong. The systematic loss of Al minerals from respirable dust may have played a significant role producing the observed trend between total silica and quartz silica dust (Fig. 7).

A determination is given on the degree of Al loss from the parent rock in the respirable dust samples. Based on elemental ratios, the Al loss from the top rock concentrations relative to Si concentrations is about 81%. Compared to Ti, elemental the loss of Al is about 87% from top rock concentrations. Since illite, kaolinite, and chlorite contain Si in additional to Al, the loss of these minerals also results in some loss of Si; meaning the Ti value is a better indicator of changes having occurred in the respirable dust fraction. It is noted that the XRF and P-7 analyses performed on the dust filters contained organic matter in the form of coal dust.

In addition to the dust and rock Si concentration lines, Fig. 7 shows two additional calculated Si rock concentration plots. The first shows the total mineral matter Si plot versus the quartz mineral matter Si plot for a pure quartz rock. Also shown is a calculated rock mineralogy with a 50% quartz and 50% clay composition. For this rock, the clay composition was assumed to be 4:1 illite to kaolinite since the XRD data suggested the clay fraction was mostly illite. The plot shows the top rock trend line to have a steeper slope than the pure quartz line. The bottom rock trend line plots very close to the 100% quartz line. Unfortunately, both the top and bottom rock plots produce trend lines with relatively low R^2 values. The quartz Si-total mineral Si line has a slope of 0.28 suggesting about 28% of the total mineral Si is present in quartz. An average top rock composition line produces a slope of about 0.88, very similar to the 50% quartz and 50% clay composition line. It is not clear why the respirable dust samples were determined to have a much smaller concentration of quartz than the potential parent rocks. The uncertain instrument

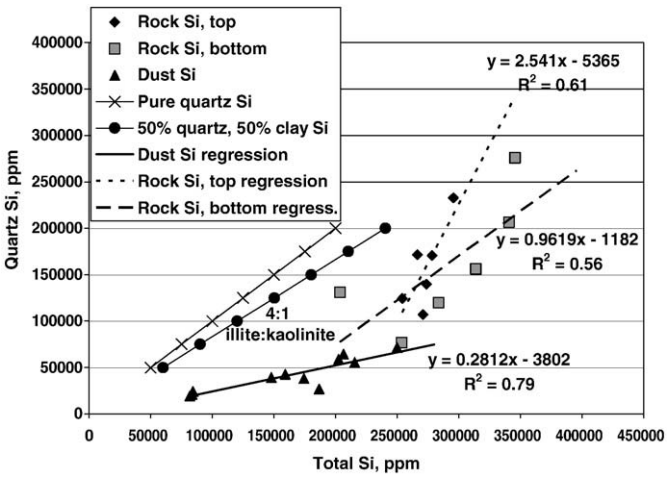

Fig. 7. Comparison of respirable dust, top and bottom rock total Si concentrations to dust, top and bottom rock quartz Si concentrations. Additional lines for rocks of 100% quartz and 50% quartz, 50% clay are shown for comparison. Dust data refers to respirable-sized particle samples.

response to mixed composition dust particles (e.g., clay and quartz) by FTIR and XRF is one potential source of error.

4. Summary and conclusions

A methodology is proposed based on alkali, alkaline earth and Mn concentrations to distinguish mine top rock strata contributions to respirable quartz dust from mine bottom rock contributions. The most consistent and pronounced cation enrichment in top rock samples was observed for Ca and Mn data. Late phase epigenetic mineralization may account for the presence of clay and lesser amounts of carbonate-bound alkali and alkaline earth minerals plus Mn with less efficient fluid transport to the bottom rock strata underlying the coal beds.

Silicon concentrations determined in respirable quartz dust were closely related to the total silicon concentrations from all mineral matter making up about an average of 28% of the sample mass. A similar relationship was not found between silicon concentrations determined in quartz and silicon concentrations from all mineral matter in the top and bottom rock. Silicate mineral matter was found to be present in the top and in the bottom rock at many sites including quartz, feldspars, illite, kaolinite and chlorite. The calculated SiO_2/Al_2O_3 and TiO_2/Al_2O_3 ratios show that the respirable dust composition has been significantly modified from the potential parent rocks. This loss of Al in the dust samples is most likely due to a disproportionately high loss of clay minerals and possibly chlorite. The preferential loss of Al-bearing minerals may account for the observed relationship between quartz Si and all mineral matter Si in respirable dust samples.

Acknowledgements

We would like to thank the following people for their valuable contributions to this research: Mr. Thomas Mal (NIOSH/PRL) for dust sample gathering and weighing and assistance at all field sites; Mr. George Persetic (NIOSH/PRL, retired) for assistance in preparing rock samples for subsequent analyses; Mr. Jay Colinet (NIOSH/PRL) for helpful input on respirable silica dust problems in coal mines; and Dr. Allan Kolker (USGS), Dr. Anthony Iannacchione (University of Pittsburgh), the late Dr. William Wallace (NIOSH/HELD), Dr. James Hower, University of Kentucky, CAER, and an anonymous reviewer for technical manuscript reviews.

Appendix A

Study sites

The three underground mining operations included in the study within West Virginia are mining the Williamson, the Lower Cedar Grove, and the Powellton coal beds (Table 1). All three of the coal beds are in the Kanawha Formation (Middle Pennsylvanian) within the Pottsville Group. In general, the Kanawha Formation coal beds contain limited mineral matter (on the order of a median value of 5% ash) and sulfur-bearing minerals (Martino, 1996).

Two Kentucky underground mining operations are included in the study. At both sites, the operators are mining the Fire Clay or Hazard No. 4 coal bed. The Fire Clay coal bed is part of the Middle Pennsylvanian Hyden Formation within the Breathitt Group. A tonstein layer (volcanic ash) is present in the lower bench of Fire Clay coal bed and is a prominent feature in the unit. Averaged data (n=24) for the Fire Clay coal bed from eastern Kentucky sites gives an ash yield of 20.22% and a sulfur content of 1.20% in the lower bench (Greb et al., 1999). Averaged data from the upper bench produced values of 7.87% for ash yield (n=39) and 1.09% sulfur content (n=44).

One coal mine site in Virginia was included in the study. This operator is mining the Lower Horsepen coal bed (Lower Pennsylvanian) which is part of the Lee or New River Formation. Abundant sandstones associated with the New River/Lee Formation coal beds are derived from eroded Alleghenian Highlands clastic matter (Cecil, 1990; Bodek and Eriksson, 2005).

Analytical methodology

All work performed on samples undergoing ICP-AES (inductively coupled plasma-atomic emission spectroscopy) including preparation and analysis was conducted by Activation Laboratories, Ltd. Entire samples were crushed to a nominal minus 10 mesh (1.7 mm), mechanically split (riffle) to obtain a representative sample and then pulverized to at least 85% minus 200 mesh (75 μm). Samples of less than 5 kg were crushed, split and pulverized with mild steel to produce samples of about 100 g. A portion of the older samples were prepared at NIOSH/PRL using a tungsten carbide shatter box, and divided into aliquots using a riffle splitter. Activision Laboratories utilizes a lithium metaborate/tetraborate fusion-ICP-AES-whole rock analysis method to dissolve the crushed samples.

Coal petrography analysis was performed by University of Kentucky, Center for Applied Energy Research (CAER). The maceral content of one or two coal samples from each mine was determined by organic petrography. All samples were completely crushed in a tungsten carbide shatterbox, and divided into aliquots using a riffle splitter. All sample preparation conducted at NIOSH was begun with a procedure very similar to American Society for Testing and Materials (ASTM) D-2013-86 (2004a). Coal petrographic samples were prepared in accordance with the requirements specified in ASTM procedure D-2797-85 (2004b). Petrographic methods are consistent with ASTM methods (2004c).

Polished mounts of coal samples from the six mine sites were analyzed using reflected-light microscopy. Analyses were performed on a Leitz (Leica) MPV compact petrographic microscope in reflected light with an oil immersion lens at a magnification of 500 times. Maceral descriptions include point counts of 1000 points on two surfaces of the polished coal pellets. The organic matter analysis included maceral point counts in accordance with current International Committee for Coal Petrography (ICCP) classification (1998, 2001). Coal rank determinations were made petrographically using vitrinite maximum and random reflectance measurements. The analyses were performed under a NIOSH contract by Dr. James Hower.

The experimental design included FTIR (Fourier transform infrared analysis) analysis of respirable dust samples by two methodologies. The analytical methods included were the MSHA P-7 protocol (Mine Safety and Health Administration, 1989) and the NIOSH 7603 procedure (National Institute for Occupational Safety and Health, 1994). The two methods were specified for a comparison of the results produced by the two techniques although the number of samples included was small. The MSHA P-7 analysis was performed by RJ LeeGroup, Inc. These measurements were performed on a Bruker Optik gmbH FTIR utilizing the Bruker Opus software version 4.2 to analyze the data.

The samples which had been planned for analysis by the NIOSH 7603 were performed by DataChem Laboratory. The samples were analyzed on a Perkin-Elmer Paragon 1000PC FTIR. To address an instrumentation irregularity, the laboratory performing the analysis modified the standard experimental method. The analytical methodology differed from NIOSH 7603 in that: samples contained on the PVC filters were treated with 9% vol/vol HCl and isopropyl alcohol; 37 mm filters instead of a 47 mm filters were used; and ashing was done in a stepwise manner instead of the described 600 °C approach. The resulting method is referred to as the P-7 alternative technique. Since the P-7 alternative results did not conform to longstanding laboratory protocols, the results may be less dependable than the MSHA P-7 data.

The X-ray fluorescence analysis was conducted by RJ LeeGroup, Inc. The samples were run on a BRUKER S4 Explorer wavelength dispersive

X-ray fluorescence (WD-XRF) unit with a gas proportional detector. The resulting spectra were analyzed using the Bruker SpectraPlus software. Respirable dust samples were analyzed by mounting filters with a Teflon backer. Raw elemental data (%) from the XRF scans were then calibrated by pure element standards (converting % to μg/cm^2).

All X ray diffraction (XRD) analysis was performed by RJ LeeGroup. The samples were run on a PANalytical X'Pert Pro MPD XRD unit is equipped with copper radiation and an X'Celerator detector from 4–64° 2-theta with a step size of 0.033°, with an overall scan time of 20 min (using the PANalytical X'Pert Pro). As previously mentioned, a low temperature ashing (LTA) procedure was performed prior to the XRD analysis.

Rock samples were removed from the field grab samples and were submitted to the lab for sample preparation and for XRD analysis. Previous research suggests that the use of LTA of coal can modify mineral matter present in typical coal samples during heating (Vassilev and Vassileva, 1996; Vassilev and Tascon, 2003). Samples were ground and mixed with a fluorite (CaF_2) known amount (~10%) internal standard. The diffraction patterns are collected using standardized scan conditions and the integrated intensities for a number of phase peaks are measured and plotted versus concentration in order to obtain a standardization factor for different diffraction peaks of the phase. A sample containing unknown proportions of mineral phases is then spiked with ~10% CaF_2, and the calibration coefficients are then used to quantify the particular mineral phase in an unknown sample. Clay analyses were done in accordance with the procedure described by Kahle et al. (2002).

The diffraction patterns were analyzed using X'Pert HighScore and DataViewer software utilizing the International Center for Diffraction Data (ICDD) database PDF2. A few of the older samples were run on a Philips XRD unit equipped with copper radiation and a graphite monochromator. These older samples were analyzed using TRACES software utilizing the ICDD database PDF2.

References

American Society for Testing and Materials, 2004a. D-2013-86 (2004): Preparation of Coal Samples for Analysis 5.05, pp. 253–263.

American Society for Testing and Materials, 2004b. D-2797-85 (1999): Preparing Coal Samples for Microscopical Determination 5.05, pp. 296–300.

American Society for Testing and Materials, 2004c. D 2799-99: Standard Test Method for Microscopical Determination of Volume Percent of Physical Components for Coal 5.05, pp. 306–309.

Bodek, R.J., Eriksson, K.A., 2005. Stratigraphic framework of the lower Pennsylvanian Lee and Pochahontas Formations in southwestern Virginia: evidence for contemporaneous trunk and tributary river systems. Geological Society of America Southern Section 54th Annual Meeting, Abstracts with Programs, vol. 37(2), p. 38.

Bohn, H.L., McNeal, B.L., O'Connor, G.A., 2002. Soil Chemistry, 3rd ed. John Wiley and Sons, New York. 307 pp.

Cecil, C.B., 1990. Paleoclimate controls on stratigraphic repetition of chemical and silicate rocks. Geology 18, 533–536.

Cecil, C.B., Stanton, R.W., Neuzil, S.G., Dulong, F.T., Ruppert, L.F., Pierce, B.S., 1985. Paleoclimate control on late Paleozoic sedimentation and peat formation in the Central Applachian Basin, USA. International Journal of Coal Geology 5, 195–230.

Chen, W., Hnizdo, E., Chen, J.-Q., Attfield, M.D., Gao, P., Hearl, F., Lu, J., Wallace, W.E., 2005. Risk of silicosis on cohorts of Chinese tin and tungsten miners and pottery workers (I): an epidemiological study. American Journal of Industrial Medicine 48, 1–9.

Dodgson, J.G., Hadden, G.G., Jones, C.O., Walton, W.H., 1971. Characteristics of the airborne dust in British coal mines. In: Walton, W.H. (Ed.), Inhaled Particles III. Unwin Brothers Ltd., Surrey, England, pp. 757–781.

Eble, C.F., Grady, W.C., 1990. Paleoecological interpretation of a Middle Pennsylvania coal bed in the central Appalachian Basin, U.S.A. International Journal of Coal Geology 16, 255–286.

Goodman, G.V., 2006. Controlling respirable dust on continuous mining operations. NIOSH/Pittsburgh Research Laboratory Research Proposal.

Greb, S.F., Eble, C.F., Hower, J.C., 1999. Depositional history of the Fire Clay coal bed (Late Duckmantian), eastern Kentucky, U.S.A. International Journal of Coal Geology 40, 255–280.

Gromet, P.L., Dymek, R.F., Haskin, L.A., Kortev, R.L., 1984. The North American shale composite: its compilation, major and minor trace element characteristics. Geochimica et Cosmochimica Acta 48, 2469–2482.

Harrison, J.C., Brower, P.S., Attfield, M.D., Doak, C.B., Keane, M.J., Grayson, R.L., Wallace, W.E., 1997. Surface composition of respirable silica particles in a set of U.S. anthracite and bituminous coal mine dusts. Journal of Aerosol Science 28, 689–696.

Harrison, J.C., Chen, J.-Q., Miller, W., Chen, W., Hnizdo, L.J., Chisolm, W., Keane, M., Gao, P., Wallace, W., 2005. Risk of silicosis on cohorts of Chinese tin and tungsten miners and pottery workers (II): workplace-specific silica particle surface composition. American Journal of Industrial Medicine 48, 10–15.

Hicks, D., Nagelschmidt, G., 1943. Special Report of the Service medical Research Council, vol. 244, pp. 153–186.

Horn, M.K., Adams, J.A.S., 1966. Computer-derived geochemical balances and abundances. Geochimica et Cosmochimica Acta 30, 279–297.

Hower, J.C., Ruppert, L.F., Eble, C.F., 1999. Lanthanide, yttrium and zirconium anomalies in the Fire Clay coal bed, Eastern Kentucky. International Journal of Coal Geology 39, 141–153.

International Committee for Coal Petrography, 1998. The new vitrinite classification (ICCP system 1994). Fuel 77, 349–358.

International Committee for Coal Petrography, 2001. The new inertinite classification system (ICCP System 1994). Fuel 80, 459–471.

Kahle, M., Kleber, M., Jahn, R., 2002. Review of XRD-based quantitative analyses of clay minerals in soils: the suitability of mineral intensity factors. Geoderma 109, 191–205.

Martino, R.L., 1996. Stratigraphy and depositional environments of the Kanawha Formation (Middle Pennsylvanian) and southern West Virginia, USA. International Journal of Coal Geology 31, 217–248.

Maynard, J.B., 1992. Chemistry of modern soils as a guide to interpreting Precambrian paleosols. Journal of Geology 100, 279–289.

Mine Safety and Health Administration, 1989. Standard Method No. P-7, Infrared Determination of Respirable Quartz in Coal Mine Dust, Internal Document. U.S. Department of Labor, Washington, D.C.

National Institute for Occupational Safety and Health, 1994. Silica, crystalline in coal mine dust, by IR, In: Eller, P.M. (Ed.), Fourth Edition. Manual of Analytical Methods, vol. 3. NIOSH, Cincinnati.

National Institute of Occupational Safety and Health, 2001. NIOSH Unpublished Analysis of Mine Safety and Health Administration Dust Compliance Data.

Ohmoto, H., 1996. Evidence in pre-2.2 Ga paleosols for the early evolution of atmospheric oxygen and terrestrial biota. Geology 24, 1135–1138.

Ramani, R.V., Mutmansky, J.M., Bhaskar, R., Qin, J., 1987. Fundamental Studies on the Relationship Between Quartz Levels in the Host Material and the Respirable Dust Generated During Mining — Volume 1: Experiments, Results and Analysis. Contract Report H058031. U.S. Bureau of Mines.

Robock, K., Bauer, H.D., 1990. Investigations into the specific fibrogenicity of mine dusts in hardcoal mines of counties of the European Community. Proc. VIIth International Pneumoconiosis Conference, Part 1: Pittsburgh, 1988. DHHS (NIOSH), pp. 280–283. publication No. 90-108, Part 1.

Rye, R., Holland, H.R., 1998. Paleosols and the evolution of atmospheric oxygen: a critical review. American Journal of Science 298, 621–672.

Schatzel, S.J., 2001. An evaluation of the origin and post-depostional modification of coal mineral matter using rare earth elements and neodymium, Pennsylvania, PhD thesis, University of Pittsburgh.

Schatzel, S.J., Stewart, B.W., 2003. Rare earth element sources and modification in the Lower Kittanning coal bed, Pennsylvania: implications for the origin of coal mineral matter and rare earth element exposure in underground coal mines. International Journal of Coal Geology 54, 223–251.

Title 30, Code of Federal Regulations, 2007. Parts 70.101, 71.101, 90.101. Office of Federal Register National Archives and Record Administration, Washington, DC, pp. 429–679.

Tuttle, M.L., 1990. Geochemistry of organic and inorganic sulfur in ancient and modern lacustrine environments. In: Orr, W.L., White, C.M. (Eds.), Geochemistry of Sulfur in Fossil Fuels. ACS Symposium Series, vol. 429, pp. 114–148.

Vassilev, S.V., Vassileva, C.G., 1996. Occurrence, abundance and origin of minerals in coals and coal ashes. Fuel Processing Technology 48, 85–106.

Vassilev, S.V., Tascon, J.M.D., 2003. Methods for the characterization of inorganic and mineral matter in coal: a critical overview. Energy and Fuels 17, 271–281.

Wallace, W.E., Harrison, J.C., Grayson, R.L., Keane, M.J., 1994. Aluminosilicate surface contamination of respirable quartz particles from coal mine dusts and clay works dusts. Inhaled Particles 7, 439–446.

Ward, C., 2002. Analysis and significance of mineral matter in coal seams. International Journal of Coal Geology 50, 134–168.

Willett, J.C., Finkelman, R.B., Mroczkowski, S., Palmer, C.A., Kolker, A., 2000. Semi-quantitative determination of the modes of occurrence of elements in coal: results from an international round robin project. In: Davidson, R.M. (Ed.), Modes of Occurrence of Trace Elements in Coal. Reports from an International Collaborative Programme. IEA Coal Research, London, UK. CD-ROM.